Electronic structure of the 2.087-eV bound exciton related to the Li_i-Li_{Ga}-O_P complex defect in GaP

Q. X. Zhao, P. Bergman, and B. Monemar
Department of Physics and Measurement Technology, Linköping University, S-58183 Linköping, Sweden
(Received 30 March 1988)

A detailed spectroscopic study of the 2.087-eV bound exciton (BE) in GaP, related to the Li_i-Li_{Ga}-O_P neutral "isoelectronic" complex defect, is presented. Zeeman data for the BE lines have been analyzed with a complete Zeeman Hamiltonian, giving accurate values for the electron-hole exchange-splitting parameter $a = 0.77 \pm 0.02$ meV and the crystal-field-splitting parameter $D = 1.66 \pm 0.02$ meV. The isotropic g values for electron and hole are evaluated as $g_e = 1.76 \pm 0.05$ and $K = 1.1 \pm 0.05$. The relative oscillator strengths for the BE substates have been computed from the Hamiltonian and the assumed wave functions, in good agreement with experimental photoluminescence excitation data, if the experimental broadening of the higher-energy BE components is accounted for. The decay times for the different BE substates have also been measured at zero field at temperatures up to 50 K and compared with expected values from the oscillator strengths.

I. INTRODUCTION

Complex defects in semiconductors are still largely an unexplored field of research, mainly due to the fact that very few such centers are positively identified (meaning that atomic and geometrical structure is known) at present. For example, only a few cases of neutral "isoelectronic" defects, where the identity is known with a large degree of confidence, exist in semiconductors; among these are the substitutional nitrogen (NN) pairs at P sites[1,2] and C_{Ga}-O_P pairs in GaP.[3–5] An even more complex defect is the Li_i-Li_{Ga}-O_P trigonal defect in GaP, which involves both substitutional and interstitial atoms. This defect was studied in early work in sufficient detail (with the aid of both O- and Li-isotope doping) so that the above-quoted identity can be regarded as well established.[6]

It appears important to investigate the few cases of complex defects where the identity is firmly established in sufficient detail, to understand the electronic structure of such defects. In early work a tentative discussion on the electronic structure of the bound exciton (BE), which constitutes the excited state of the Li_i-Li_{Ga}-O_P defect at low temperature, was given,[6] based on luminescence spectroscopy, including Zeeman data taken up to 3.2 T. Although the data presented in Ref. 6 can be regarded as accurate, the analysis was incomplete, and good agreement with the theoretical model for the electronic structure was not obtained. In this work we have repeated the Zeeman data reported by Dean,[6] with very good agreement. We have employed a sufficiently complete Hamiltonian for the BE, together with simple but realistic basis functions for the bound electrons and holes, to analyze the Zeeman data.[7] This gives reliable values for the electron-hole (e-h) exchange-splitting parameter a, and also the local-field splitting parameter D for the bound-hole states. The g values for both electron and hole are also obtained accurately. Consequently, a complete set of accurate parameters for the electronic structure has been obtained for the first time for such a complicated defect, composed of three impurity atoms. This defect is a model complex neutral defect in trigonal symmetry, with a dominantly electron-attractive potential, caused by the deep substitutional O_P donor being part of the defect.[8–10]

By employing a tunable dye laser, photoluminescence excitation (PLE) spectra[11] could be used in this work to measure the relative oscillator strengths of the observed BE substates for the Li_i-Li_{Ga}-O_P defect. These data were compared with a simulated spectrum, obtained with the aid of the employed zero-field Hamiltonian, and the wave functions derived for the BE substates. In addition, transient measurements were performed, detecting the decay of the BE emission with excitation from a mode-locked dye laser. These data can be explained within the model for the electronic structure derived from the Zeeman data.

The paper is organized in the following way. In Sec. II we give a brief description of samples and experimental procedures. In Sec. III the theoretical formalism used in the evaluation of the data is discussed, i.e., the BE Hamiltonian and the wave functions. Section IV contains the experimental results from the various measurements with laser spectroscopy, including Zeeman, PLE, and transient PL data. In Sec. V, finally, a discussion of the data is provided, with reference to the theoretical framework developed in Sec. III.

II. SAMPLES AND EXPERIMENTAL PROCEDURE

The GaP samples used in this work were small solution-grown platelets. Originally they were nominally undoped, but contained residual impurities such as S, Si, N, and O in concentrations estimated to be around 10^{16} cm^{-3}. Li doping was performed with a one-step diffusion process in evacuated quartz ampoules. The diffusion source was Li-metal pellets, which were placed on a

 ©1988 The American Physical Society

quartz support plate inside the ampoule, to avoid attack from the Li directly on the wall of the ampoule. Typical diffusion temperatures ranged from 600 to 800 °C, during 1 h.

For the photoluminescence measurements an exchange-gas He cryostat was employed, where the sample temperature could be accurately regulated between 1.5 and 300 K. For the stationary PLE experiments a Coherent 590 dye laser with a Rhodamine-6G dye was employed. Spectra were obtained with either an S-20 type or a GaAs-type photomultiplier, together with a Spex 1404 0.85-m double-grating monochromator. Zeeman data were obtained with an Oxford Spectramag 4 superconducting magnet in the Voigt configuration and at fields up to 7 T. PL transients were obtained with a time-correlated photon-counting system, where the luminescence was detected with a cooled GaAs photomultiplier tube. The laser system used for the pulsed excitation consisted of a Coherent Innova 100 mode-locked argon-ion laser together with a dye laser and a cavity dumper. The time resolution of the system was better than 1 ns, which is much shorter than any of the measured decay times. The excitation was made both resonant with the BE energy levels, and at higher photon energies, but always below the band gap.

III. THEORETICAL FRAMEWORK FOR THE ELECTRONIC STRUCTURE OF A BOUND EXCITON ASSOCIATED WITH AN ELECTRON-ATTRACTIVE NEUTRAL DEFECT

For an electron-attractive neutral "isoelectronic" defect the relevant bound-exciton Hamiltonian $H_{\rm BE}$ in GaP typically involves a spinlike ($s_e=\frac{1}{2}$) electron and a p-like ($J_h=\frac{3}{2}$) hole.[12–14] Including external perturbations, $H_{\rm BE}$ can be written[7]

$$H_{\rm BE}=H_0+H_1 , \tag{1}$$

where H_0 is the zero-field Hamiltonian and H_1 represents the external perturbation field. In this case H_0 has two dominant terms; one of them is the e-h exchange interaction

$$H_{\rm ex}=-a\mathbf{J}_h\cdot\mathbf{s}_e , \tag{2}$$

where $\mathbf{J}_h$ represents the total angular momentum of the bound hole, while $\mathbf{s}_e$ is the corresponding quantity for the electron. The other term represents the influence of the local crystal field on the bound hole, which for a low-symmetry defect can be written[7,13–16]

$$H_{\rm LCF}=-D[J_{hz'}^2-\tfrac{1}{3}J_h(J_h+1)]-E(J_{x'}^2-J_{y'}^2) . \tag{3}$$

Here the set of axes (x',y',z') refer to the local defect axes, while x,y,z refer to the cubic axes of the crystal. Further, E is nonzero for a defect symmetry lower than trigonal. For trigonal symmetry, as appropriate in this work, only the first term in Eq. (3) needs to be considered.[7]

If the external field is a magnetic field, H_1 denotes the Zeeman Hamiltonian. It can be divided into the linear term

$$H_{\rm LZ}=\mu_B[g_e\mathbf{B}\cdot\mathbf{s}_e+K\mathbf{B}\cdot\mathbf{J}_h+L(B_xJ_{hx}^3+B_yJ_{hy}^3+B_zJ_{hz}^3)] \tag{4}$$

and the quadratic term

$$H_{\rm QZ}=C_1B^2+C_2(\mathbf{J}_h\cdot\mathbf{B})^2 . \tag{5}$$

The total Hamiltonian $H_{\rm BE}$ in the presence of an external magnetic field can therefore be written

$$H_{\rm BE}=H_{\rm ex}+H_{\rm LCF}+H_{\rm LZ}+H_{\rm QZ} , \tag{6}$$

with the terms given explicitly in Eqs. (2)–(5) above.

In order to use this Hamiltonian in connection with experimental data, suitable wave functions for electrons and holes have to be used. In the case studied here the Γ_8 basis set ($J=\frac{3}{2}$) for the bound hole is appropriate, if the hole is shallow and effective-mass- (EM) like.[7,13–17] For the spinlike electron a simple $s=\frac{1}{2}$ basis is considered appropriate,[7,13–16] even for strong localization. As long as absolute values of matrix elements are not computed, the details of the radial parts of the wave functions need not be considered. The Hamiltonian $H_{\rm BE}$ is diagonalized with this basis set, which yields explicit eigenenergies and wave functions for the BE substates, which are split by the local and external fields.[7] Without external field, explicit expressions can be derived for the eigenenergies and wave functions.[7,17] In the general case [Eq. (6)] a numerical technique has to be employed, as discussed in Ref. 7. A computer program was developed to perform the fit of the theoretical model to the data, including at least-squares-fitting procedure.

In the case studied in this work, it is possible to derive explicit expressions for the BE zero-field substates, which are split by the e-h exchange interaction and the local crystal field. In Ref. 7 such explicit expressions for the BE energy levels were derived for C_{2v} symmetry, and the corresponding expressions for C_{3v} symmetry, as appropriate for the Li_i-$\mathrm{Li}_{\rm Ga}$-$\mathrm{O}_{\rm P}$ defect, are easily obtained with the aid of Eq. (9) in Ref. 7:

$$\begin{aligned}
&E(J=1;\,m=0)=\tfrac{5}{4}a+D ,\\
&E(J=1;\,m=\pm1)=a/4+(D^2-aD+a^2)^{1/2} ,\\
&E(J=2;\,m=0)=-\tfrac{3}{4}a+D ,\\
&E(J=2;\,m=\pm1)=a/4-(D^2-aD+a^2)^{1/2} ,\\
&E(J=2;\,m=\pm2)=-\tfrac{3}{4}a-D .
\end{aligned} \tag{7}$$

Similar expressions were derived in Ref. 17 (where the notations used can be translated as $D=\epsilon_0$, $2a=\Delta$).

Once the eigenfunctions for the BE substates have been obtained, oscillator strengths for optical transitions between the BE substates and the ground state (with no particles bound) can be calculated. Such oscillator strengths are proportional to the square of the electric dipole matrix element:

$$M_{i0}=\langle\psi_i\,|\,\mathbf{Q}\,|\,\psi_0\rangle , \tag{8}$$

where $\mathbf{Q}$ is the dipole transition operator, ψ_i is a particu-

lar BE substate, and ψ_0 is the BE ground state. Such computed oscillator strengths are a critical test of the adequacy of the assumed model for the Hamiltonian and, in particular, for the chosen basis set.[7]

IV. EXPERIMENTAL DATA COMPARED WITH THE THEORETICAL MODEL FOR THE ELECTRONIC STRUCTURE

The zero-field PL spectrum of the 2.087-eV BE is shown in Fig. 1 at two different temperatures, for easy reference. Similar PL spectra were also presented in great detail in Figs. 1 and 2 of Ref. 6, and our spectral PL data are in complete agreement. We note, however, that in our samples the thermal quenching of the BE occurred at much higher temperatures (about 200 K) than reported by Dean ($\approx$77 K).[6]

Experimental Zeeman data were obtained for fields up to 7 T including a full angular dependence in a (110) plane. Since the natural linewidths of the BE PL lines in our case were broader than in the data previously published by Dean,[6] the set of data summarized in Fig. 5 of Ref. 6 for $B=3.2$ T were actually of similar accuracy as our data obtained for 7 T. To illustrate the development made here in comparison with the Dean's work,[6] we have therefore chosen to show a fit of the data from Fig. 5 in Ref. 6 with a complete Zeeman Hamiltonian [Eq. (6)]. The result is shown in Fig. 2 for the fan diagram, i.e., the development of the energies of the BE substrates with applied magnetic field along one direction, in this case [100]. Figure 3 shows the angular dependence of the Zeeman splittings, with the magnetic field **B** rotated in a (110) plane. The lines shown in Figs. 2 and 3 are obtained from a best fit of the Hamiltonian in Eq. (6) to the data (shown as dots), with the resulting parameters given in Table I.

The set of PL Zeeman data just described only includes the two lowest zero-field BE lines, due to thermalization in the PL spectra. Figure 4(a) shows a PLE spectrum obtained at 2 K, with detection in the LO-phonon replica, showing all the BE transitions, with strengths proportional to the respective oscillator strengths. As a comparison, shown in Figs. 4(b) and 4(c) are the theoretically simulated PLE spectra, using the same zero-field parameters a and D as derived from the Zeeman data (Table I), but with different broadening for the higher-energy BE sublevels. A good agreement is obtained between theory and experiment, if the different broadening observed for the different BE transitions is properly accounted for in the comparison.

The PLE spectrum for the 2.087-eV BE was obtained over a wide photon-energy region above the electronic BE lines, as partly shown in Fig. 5. The structure observed above the electronic lines can be identified as due to various quasilocalized phonon modes, which are also observed in PL emission (Fig. 1 and Ref. 6). An interesting observation is the apparent absence of any discrete lines due to single-particle excitations of the shallow bound hole of the BE, as has been previously observed, e.g., for the NN BE's in GaP.[2] The strong phonon coupling for the 2.087-eV BE may be the reason these transitions are not observed in this case.

The measured values of the decay time as a function of temperature are shown in Fig. 6; the circles correspond to values obtained with resonant excitation. The detection of PL was done in the BE phonon wing about $\approx$50 meV during the BE states. No difference in the decay time was observed during resonant excitation in the $J=1$ and 2 substates, respectively. The squares correspond to

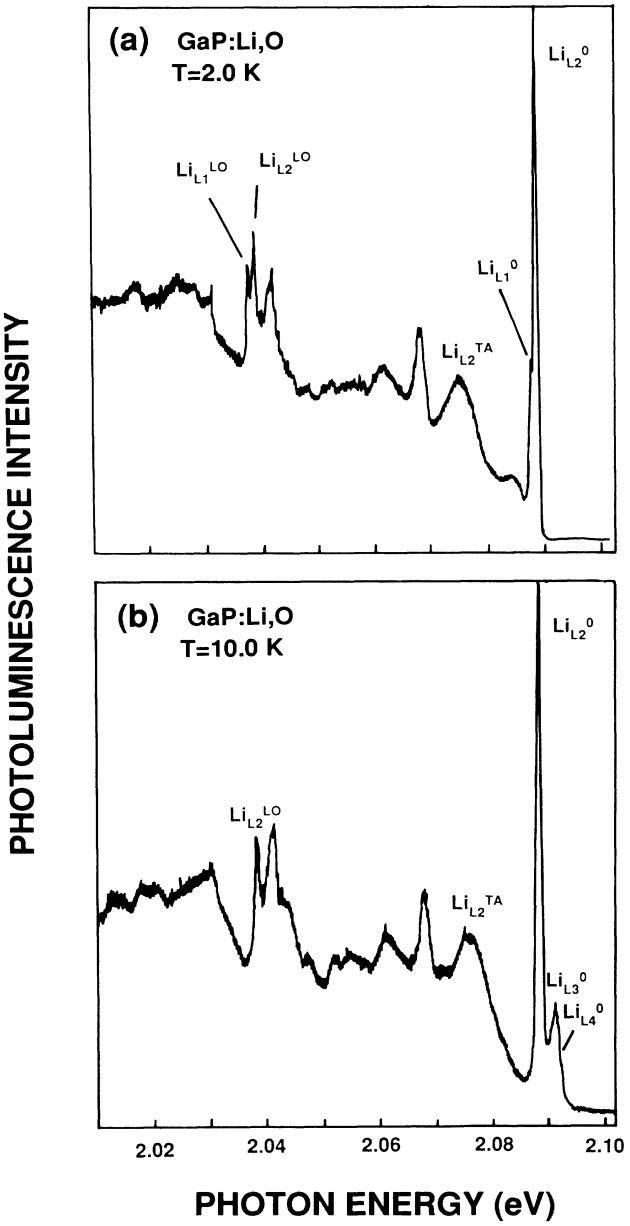

FIG. 1. Photoluminescence spectrum of the 2.087-eV bound exciton in GaP, obtained at two temperatures, (a) 2 K and (b) 10 K, with 5145-Å Ar^+-laser excitation. In the low-temperature spectrum (a), the two lowest electronic lines Li_{L1}^0 and Li_{L2}^0 are resolved, together with a broad phonon wing. At 10 K, panel (b), the weak Li_{L1}^0 line is not seen, while now, in addition to the strong Li_{L2}^0 line, the broadened Li_{L3}^0 and Li_{L4}^0 transitions also appear. The rich spectrum of phonons coupling to the electronic lines is discussed in detail in Ref. 6.

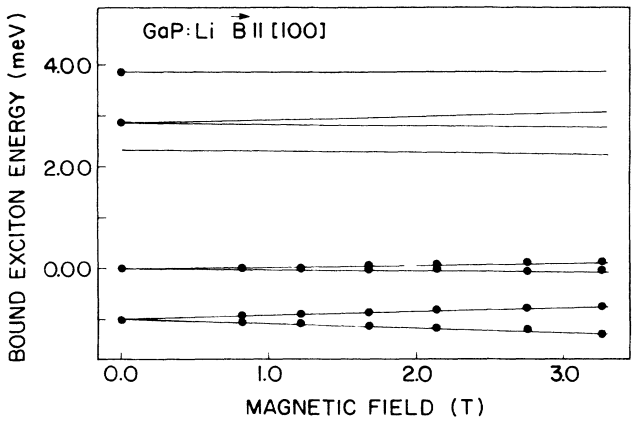

FIG. 2. Fan diagram for the splitting of the 2.087-eV bound-exciton sublevels with magnetic field, ranging from $B=0$ T to $B=3.2$ T, in the [001] direction. Solid lines are computer simulated from the spin Hamiltonian given in the text [Eq. (6)], while the experimental points are taken from the data in Ref. 6.

values measured in the BE $J=2$ no-phonon line, with the excitation 30 meV above.

The decay curves are exponential at temperatures up to 30 K, as shown in Fig. 7; above this temperature a nonexponential decay is observed. This is partly due to an overlapping emission with much longer decay time which becomes relatively stronger compared to the Li-Li-O BE emission at high temperatures. Whether this overlapping emission is connected to the Li_i-Li_{Ga}-O_P center has not been established. The measured values of the decay time as a function of temperature are in agreement with the values obtained in Ref. 6, measured only at two different temperatures, $\tau=200$ and 720 ns at 20 and 4.2 K, respectively.

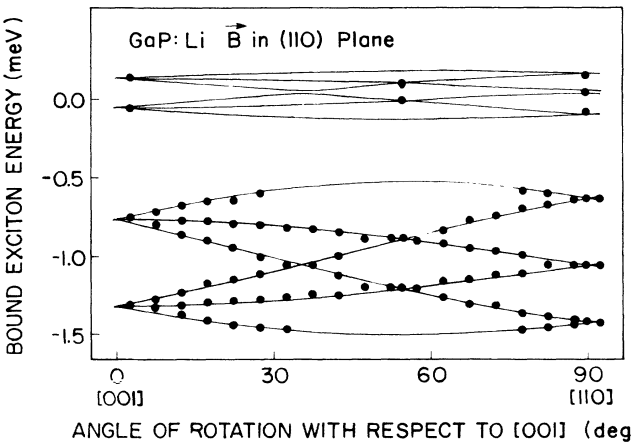

FIG. 3. Angular dependence of the Zeeman splitting of the 2.087-eV bound exciton obtained at 2 K with $B=3.2$ T in the Voigt configuration. Only the two lowest BE sublevels can be studied at 2 K. The magnetic field **B** is rotated in the $(1\bar{1}0)$ plane. Solid lines are computer simulated from the spin Hamiltonian given in the text [Eq. (6)]. The experimental points are taken from the data in Ref. 6.

TABLE I. Synopsis of the parameters in the perturbation Hamiltonian describing the Zeeman splitting of the 2.087-eV Li_i-Li_{Ga}-O_P–related bound exciton. The error bars are entirely due to the observed width of the higher-energy BE lines.

$a=0.77\pm0.02$ meV
$D=1.66\pm0.02$ meV
$g=1.76\pm0.05$
$K=1.1\pm0.05$
$L=0$
$C_1=C_2=0$

By assuming thermal equilibrium between the different BE substates, which is obtained if the spin-lattice relaxation time is faster than any of the characteristic radiative recombination times of the BE substates, it is possible to express the measured decay time as a function of temperature according to

$$\tau=\frac{\sum_i g_i e^{-(E_i-E_1)/kT}}{\sum_i \frac{g_i}{\tau_i} e^{-(E_i-E_1)/kT}}, \tag{9}$$

where the label $i=1-5$ corresponds to the different substates counted from lower energy. g_i, E_i, and τ_i are the degeneracy, energy, and radiative lifetime of each substate, respectively.

It is not possible, however, to make a complete fit of the measured values to Eq. (9), due to thermal quenching of the total luminescence. This quenching can be viewed as a fast thermally activated, nonradiative recombination which decreases the observed luminescence decay time. Unfortunately, this is happening in the same temperature range where the higher-energy substates become thermally populated. The equation above must be adjusted with a term for the thermal quenching, which gives two new parameters. It is not meaningful to fit the data to an equation with seven parameters. It is possible, however, to fit the data at low temperatures where the thermal quenching as well as the three higher-energy substates can be neglected. The best fit is obtained for $\tau_1=2500$ ns and $\tau_2=100$ ns. The curve corresponding to these values are inserted into Fig. 6 as a solid line.

The lifetimes τ_1 and τ_2 are inversely proportional to the oscillator strength of the particular substates, and the ratio of the oscillator strength between the allowed $m=\pm1$ $(J=2)$ and the forbidden $m=\pm2$ $(J=2)$ state is thus found to be 25.

V. DISCUSSION

The parameters for the zero-field Hamiltonian in this case, i.e., a and D, could be obtained from the computer fit of the Zeeman data with the complete Hamiltonian [Eq. (6)]. From an inspection of the Zeeman data and the zero-field PLE spectra, it is obvious that $D>0$, and then Eq. (7) gives an explicit solution for D and a, using the measured energy positions of the BE zero-field substates:

$E(J=2; m=\pm1)-E(J=2; m=\pm2)=0.99$ meV and $E(J=1; m=\pm1)-E(J=2; m=\pm2)=3.86$ meV. Inserting these values in Eq. (7), two sets of values can be obtained ($a=0.77$ meV, $D=1.66$ meV) and ($a=1.66$ meV, $D=0.77$ meV), respectively. Only the first set of these values is consistent with the oscillator strengths,

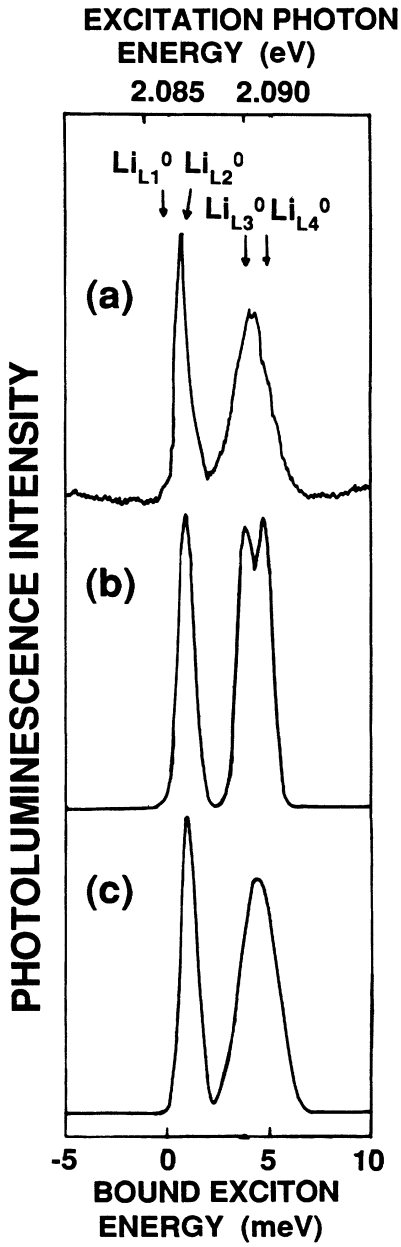

FIG. 4. (a) Photoluminescence-excitation (PLE) spectrum of the 2.087-eV bound exciton, obtained at 2 K with a tunable dye laser. Detection is in the LO-phonon replica of the bound exciton (see Fig. 1). The energy position of the different electronic sublevels, as obtained from PL data (Fig. 1), are shown at the top. The bound-exciton energy scale at the bottom is a relative energy scale, with the zero point taken at Li_{L1}^0. (b) Theoretically simulated spectrum, as described in the text [Eq. (8)], with the same Gaussian broadening, $\sigma=0.38$ meV, applied to all sublevels. (c) Same as in (b), but with a different Gaussian broadening for different sublevels: $\sigma_2=0.38$ meV for the $J=2$ sublevels and $\sigma_1=0.7$ meV for the $J=1$ sublevels, respectively.

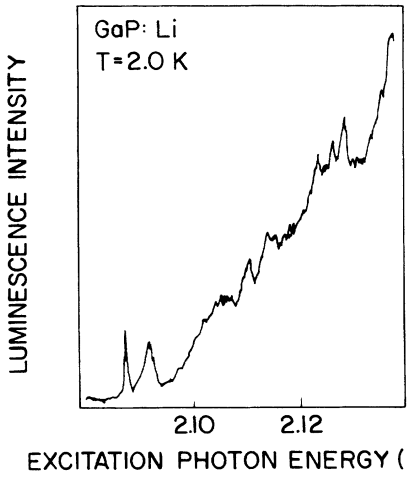

FIG. 5. PLE spectrum as in Fig. 4(a), but for a more extended photon-energy region, covering the one-phonon sideband in absorption for the 2.087-eV BE. The structure above the electronic lines can be identified with a variety of different quasilocalized phonon modes, as also observed in PL emission spectra (Fig. 1 and Ref. 6). No single-particle–excited hole states are observed.

however, as seen in Fig. 4. Hence, once the different substates are identified by Zeeman measurements, the computer evaluation of the zero-field parameters can be avoided in this simple trigonal symmetry.

The electronic structure of the 2.087-eV BE is summarized in Fig. 8, which is drawn in a scale proper for the experimentally observed energies for the BE sublevels. The development of the sublevel splittings for the

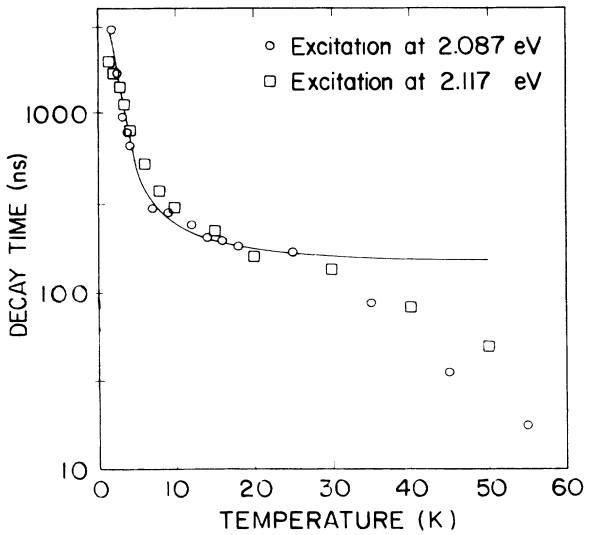

FIG. 6. The photoluminescence spectra of the 2.087-eV BE system, plotted as a function of temperature. The circles correspond to data obtained with resonant excitation in the $J=1$ BE lines, while squares are obtained with nonresonant below-band-gap excitation. The solid line represents the theoretical simulation according to Eq. (9).

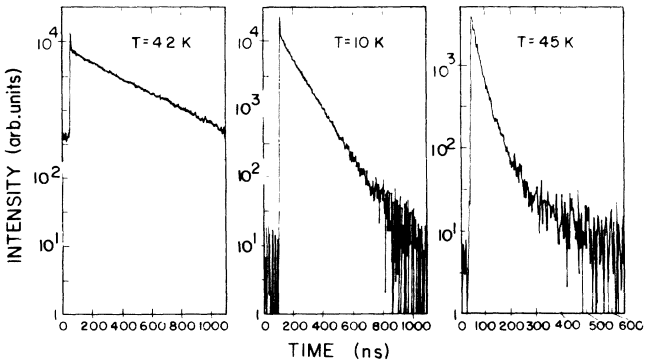

FIG. 7. The observed decay curves for the 2.087-eV BE, at three different temperatures: (a) $T=2$ K, (b) $T=10$ K, and (c) $T=45$ K. The intensity is given on a logarithmic scale.

relevant value of the *e-h* exchange interaction is illustrated.

Although the data obtained for the 2.087-eV BE in the previous work by Dean[6] were in excellent agreement with our data, the analysis presented in Ref. 6 was oversimplified, yielding an overly small value for the a parameter, while the D value was similar. It was also noted in Ref. 6 that the derived values for a and D did not give a good fit to the observed relative oscillator strengths of the BE substates, and the geometrical model for the defect was therefore questioned.[6] The simplified analysis of the Zeeman data in Ref. 6 yielded values for g_e and K in good agreement with our data, obtained from the full Zeeman Hamiltonian, although the error bars on these parameters could be reduced in the present work. The reason of the success of the earlier analysis for the magnetic parameters[6] is that in the high-symmetry (trigonal) crystal field the $m_J=\pm 2$ ($J=2$) quantum numbers can be regarded as proper, so the procedure used in Ref. 6 for evaluating g_e and K using these states gives approximately correct values. The same procedure is not possible to use in the fitting of the $m=\pm 1$ ($J=2$) substates,

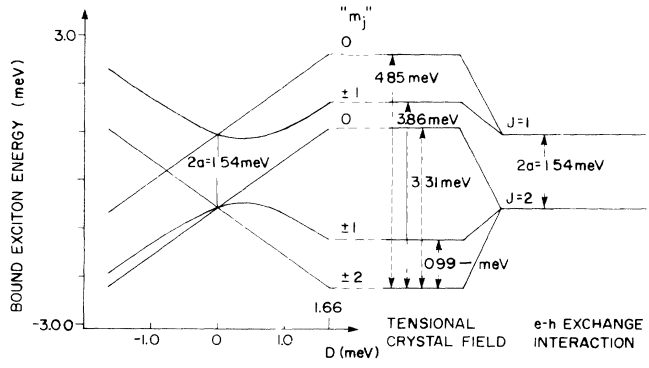

FIG. 8. To the left is shown a plot of the bound-exciton energy vs crystal field for a trigonal crystal field, relevant for the 2.087-eV BE. To the right the electronic structure is drawn for this BE, including the sublevel energies, as obtained from experimental data in this work.

since these mix strongly with the higher $m=\pm 1$ ($J=1$) substates. Therefore the use of a complete Hamiltonian, as done in this work, is the proper way to analyze the Zeeman data presented in Figs. 1 and 2.

The value of K is typical for shallow hole states in GaP, such as, e.g., in BE's bound to substitutional donors.[18] The fact that the constants C_1 and C_2 in Eq. (5) were found to be zero in this case is strong evidence that the electron is strongly localized, as already concluded by Dean.[6] This defect therefore constitutes another example of the validity of the Hopfield-Thomas-Lynch[19] model for an isoelectronic defect. The g_e value 1.76 ± 0.05 is considerably reduced compared to the value 2.00 found for most shallow donors, and also expected for very localized electrons. It seems that a strongly-electron-attractive low-symmetry potential in GaP gives rise to a g_e value for the bound electron that is significantly reduced below 2.00. A similar observation was made for the $(NN)_1$ BE ($g_e=1.85$, Ref. 7). Such a reduction cannot be predicted by simple arguments, since it must be calculated via deep-level theory for the localized electron state.

The fit of relative oscillator strengths presented in Fig. 4 is encouraging, since it gives a good agreement with experiment if a larger broadening of the higher BE substates is accounted for in the comparison. In earlier work no such agreement was obtained.[6] This agreement gives confidence that the Hamiltonian used is realistic for describing a BE at a complex defect with a dominantly-electron-attractive local potential. Further, the simple basis set chosen must also be realistic, as may be expected if the hole is EM-like. For EM-like holes the p-like Bloch functions characteristic of the valence-band top[20] should be a reasonable approximation of the wave functions. Details of the spatial parts of the BE wave functions are not discussed here, since they occur as common factors in the evaluation of relative oscillator strengths.

The conclusion that O_P dominates the defect potential for the Li_i-Li_{Ga}-O_P complex is maybe not surprising, considering the strong potential of the deep O_P donor, which gives a one-electron state at 0.90 eV,[8-10] and, in addition, can bind a second electron in another deep state (0.57 eV).[21] Li_i is known to be a shallow donor at tetrahedral interstitial sites,[22,23] while Li_{Ga} is probably a quite deep double acceptor,[24] not yet positively identified. It appears that the presence of a Li_i close to Li_{Ga} reduces this acceptor potential to a large degree, so that O_P is by far the dominating impurity potential in the complex. This is similar to the previously studied case with the trigonal Zn_{Ga}-O_P and Cd_{Ga}-O_P complexes in GaP,[3-5] which both have a BE with a shallow EM-like hole.[5] The fact that the Li_i-Li_{Ga}-O_P BE is slightly shallower than the Cd-O- and Zn-O-related BE's can be understood by a somewhat larger cancellation between the Li_{Ga} and O_P potentials, which is expected since Zn_{Ga} and Cd_{Ga} are shallow acceptors in GaP.[25]

The observed large broadening (≈ 0.5 meV) of the high-energy BE substrates $Li^0_{3,4}$ (Fig. 3) is interesting, and consistent with similar observations on the GaP:$(NN)_1$ BE (Ref. 7) and the 1.429-eV BE in GaAs (Ref. 15). Two

effects may be important in causing this broadening. One of them is a lifetime broadening due to a fast spin-lattice relaxation time for the high-energy substates. It is noted that for the $J=1$ substate of the GaP:N BE at 2.318 eV a short relaxation time of about 25 ps has been measured.[26] Another contribution could be a broadening due to spectral overlap with a rather strong background originating from the coupling of the lower-energy BE lines to acoustic phonons in the optical-absorption process.

VI. CONCLUSIONS

This work presents an improved analysis in the previous work of Dean[6] on the Li_i-Li_{Ga}-O_P defect in GaP, spectroscopically observed via the 2.087-eV bound exciton. The Zeeman data are complemented by novel measurements of photoluminescence-excitation spectra and transient decay times in this work. The analysis uses a proper Zeeman Hamiltonian, with an adequate treatment of the zero-field part. The values derived for the exchange parameter $a=0.77$ meV is substantially larger than that estimated by Dean ($\Delta=2a=1.1$ meV), while the local-field parameter D is similar. We find $D=1.65$ meV, while the earlier value was given as $2\epsilon_0=2D=3.4$ meV.[6]

In addition to PL and PLE data, relative oscillator strengths for the BE substates have been computed, and compared favorably with the experimental PLE data, in contrast to what was found in earlier work. A large broadening of the upper BE sublevels is observed, probably due to a short spin-lattice relaxation time and also a rather strong phonon coupling for this BE. The measured decay times are in agreement with the observed relative oscillator strengths, assuming a short spin-lattice relaxation time.

The accurate evaluation of magnetic data ($g_e=1.76$, $K=1.1$, $C_1=C_2=0$) provided here confirms the model of a strongly localized electron and a shallow effective-mass-like hole for this BE. The reduced g_e value for such a case in a low-symmetry potential is interesting and calls for theoretical investigations.

[1]D. G. Thomas and J. J. Hopfield, Phys. Rev. **150**, 680 (1966).
[2]E. Cohen and M. D. Sturge, Phys. Rev. B **15**, 1039 (1977).
[3]P. J. Dean, in *Applied Solid State Sciences*, edited by R. Wolfe (Academic, New York, 1970), Vol. 1, p. 1.
[4]T. N. Morgan, B. Welber, and R. N. Bhargava, Phys. Rev. **166**, 751 (1968).
[5]C. H. Henry, P. J. Dean, and J. C. Cuthbert, Phys. Rev. **166**, 754 (1968).
[6]P. J. Dean, Phys. Rev. B **4**, 2596 (1971).
[7]Q. X. Zhao and B. Monemar, Phys. Rev. B **38**, 1397 (1988).
[8]P. J. Dean, C. H. Henry, and C. J. Frosch, Phys. Rev. **168**, 812 (1968).
[9]P. J. Dean and C. H. Henry, Phys. Rev. **176**, 928 (1968).
[10]B. Monemar and L. Samuelson, Phys. Rev. B **18**, 809 (1978).
[11]B. Monemar, H. P. Gislason, P. J. Dean, and D. C. Herbert, Phys. Rev. B **25**, 7719 (1982).
[12]B. Monemar, U. Lindefelt, and M. E. Pistol, J. Lumin. **36**, 149 (1986).
[13]B. Monemar, U. Lindefelt, and W. M. Chen, Physica B + C **146B**, 256 (1987).
[14]B. Monemar, CRC Crit. Rev. Solid-State Sci. (to be published).
[15]P. O. Holtz, Q. X. Zhao, and B. Monemar, Phys. Rev. B **36**, 5051 (1987).
[16]W. M. Chen and B. Monemar (unpublished).
[17]J. van W. Morgan and T. N. Morgan, Phys. Rev. B **1**, 739 (1970).
[18]P. J. Dean, D. Bimberg, and F. Mansfeld, Phys. Rev. B **15**, 3906 (1977).
[19]J. J. Hopfield, D. G. Thomas, and R. T. Lynch, Phys. Rev. Lett. **17**, 312 (1966).
[20]A. Baldereschi and N. O. Lipari, Phys. Rev. B **3**, 439 (1971).
[21]P. J. Dean, in *Deep Centers in Semiconductors*, edited by S. T. Pantelides (Gordon and Breach, New York, 1986), p. 185.
[22]P. J. Dean, in *Proceedings of the International Conference on Luminescence, Leningrad, 1972*, edited by F. Williams (Plenum, New York, 1973), p. 538.
[23]M. Godlewski, W. M. Chen, and B. Monemar, Phys. Rev. B **33**, 8246 (1986).
[24]W. M. Chen, Ph.D. thesis, Linköping University, 1986.
[25]W. Berndt, A. A. Kopylov, and A. N. Pikhtin, Pis'ma Zh. Eksp. Teor. Fiz. **22**, 578 (1975) [JETP Lett. **22**, 284 (1975)].
[26]L. W. Molenkamp and D. A. Wiersma, Phys. Rev. B **32**, 8108 (1985).